Talanta 115 (2013) 159–165

Contents lists available at ScienceDirect

Talanta

journal homepage: www.elsevier.com/locate/talanta

An aptamer-based bio-barcode assay with isothermal recombinase polymerase amplification for cytochrome-*c* detection and anti-cancer drug screening

Jacky F.C. Loo [a], P.M. Lau [a], H.P. Ho [b], S.K. Kong [a,*]

[a] The Chinese University of Hong Kong, School of Life Sciences, Biochemistry Programme, Room 609, Mong Man Wai Building, Shatin, NT, Hong Kong
[b] Center for Advanced Research in Photonics, Department of Electronic Engineering, The Chinese University of Hong Kong, Shatin, NT, Hong Kong

ARTICLE INFO

Article history:
Received 11 January 2013
Received in revised form
18 April 2013
Accepted 22 April 2013
Available online 28 April 2013

Keywords:
Aptamer
Anti-cancer drug screening
Bio-barcode assay
Polyphyllin *D*

ABSTRACT

Based on a recently reported ultra-sensitive bio-barcode (BBC) assay, we have developed an aptamer-based bio-barcode (ABC) alternative to detect a cell death marker cytochrome-*c* (Cyto-*c*) and its subsequent application to screen anti-cancer drugs. Aptamer is a short single-stranded DNA selected from a synthetic DNA library by virtue of its high binding affinity and specificity to its target based on its unique 3D structure from the nucleotide sequence after folding. In the BBC assay, an antigen (Ag) in analytes is captured by a micro-magnetic particle (MMP) coated with capturing antibodies (Abs). Gold nanoparticles (NPs) with another recognition Ab against the same target and hundreds of identical DNA molecules of known sequence are subsequently added to allow the formation of sandwich structures ([MMP-Ab1]-Ag-[Ab2-NP-DNA]). After isolating the sandwiches by a magnetic field, the DNAs hybridized to their complementary DNAs covalently bound on the NPs are released from the sandwiches after heating. Acting as an Ag identification tag, these bio-barcode DNAs with known DNA sequence are then amplified by polymerase chain reaction (PCR) and detected by fluorescence. In our ABC assay, we employed a Cyto-*c*-specific aptamer to substitute both the recognition Ab and barcode DNAs on the NPs in the BBC assay; and a novel isothermal recombinase polymerase amplification for the time-consuming PCR. The detection limit of our ABC assay for the Cyto-*c* was found to be 10 ng/mL and this new assay can be completed within 3 h. Several potential anti-cancer drugs have been tested *in vitro* for their efficacy to kill liver cancer with or without multi-drug resistance.

1. Introduction

Cancer is a disease characterized by uncontrolled cell growth and proliferation. It is a major health problem worldwide to date. During chemo- and radio-therapy, some cancer cells develop resistance against structurally and functionally unrelated anti-cancer drugs. This so-called multi-drug resistance (MDR) phenomenon is now a major factor in the failure of many forms of cancer treatment [1]. The search for novel and effective anti-cancer agents against cancers with MDR is therefore a matter of urgency.

Now, it is widely reported that the killing of cancer cells by anti-cancer drugs is predominantly mediated by apoptosis [2] and the release of cytochrome-*c* (Cyto-*c*) from the mitochondria into the cytosol of the cancer cells is a key mediator that triggers the final steps of apoptosis such as caspase-3 activation and DNA fragmentation [3,4]. Because of this, release of Cyto-*c* from the mitochondria is regarded as a 'point-of-no-return' stage in the cell death pathway [5]. Moreover, the release of Cyto-*c* is an early event and it is readily detectable in the culture medium of apoptotic cells, thereby making it an important and effective biomarker for the efficacy of potential anti-cancer agents for killing cancer [4,6]. Conventionally, the amount of Cyto-*c* released from cells can be determined by the enzyme-linked immunosorbent assay (ELISA). Unfortunately, nearly all of the antibodies (Abs) against Cyto-*c* do not show a single band in the Western blot analysis, thus indicating the cross-reactivity of the anti-Cyto-*c* Ab that binds to some other proteins. Also, the signal amplification in ELISA is mediated by enzymatic reaction that is limited by the availability of substrates. Alternatively, Cyto-*c* can be detected by the Western blot analysis. The merit of this approach is that two

Abbreviations: Ab, Antibody; ABC assay, Aptamer-based bio-barcode assay; BBC assay, Bio-barcode assay; Cyto-*c*, Cytochrome-*c*; ELISA, Enzyme-linked immunosorbent assay; MDR, Multi-drug resistance; MMP, Micro-magnetic particle; NP, Nanoparticle; PCR, Polymerase chain reaction; PD, Polyphyllin D; RPA, Recombinase polymerase amplification; SELEX, Systematic evolution of ligands by exponential enrichment; $\Delta\Psi_m$, Mitochondrial trans-membrane potential.

* Corresponding author. Tel.: +852 3943 6799; fax: +852 2603 7246.
E-mail address: skkong@cuhk.edu.hk (S.K. Kong).

0039-9140/$ - see front matter © 2013 Elsevier B.V. All rights reserved.
http://dx.doi.org/10.1016/j.talanta.2013.04.051

parameters, the molecular size resolved by the gel electrophoresis and immuno-specificity from the Ab–Ag reaction, are used to confirm the amount of the target of interest [7]. Apart from being tedious, troublesome and time-consuming, this technique is an end-point approach. In order to have a fast sample turn-around speed for drug screening including that for anti-cancer agent searching, we report here a new aptamer-based bio-barcode (ABC) assay for rapid Cyto-*c* detection adopting the principle form the well-known ultra-sensitive bio-barcode (BBC) assay.

In 2003, Mirkin and his coworkers developed an extraordinarily sensitive immunoassay called BBC assay that has a detection limit up to attomolar level (10^{-18} M) [8–10]. In the BBC assay, two particles are used. The first is a micro-magnetic particle (MMP) coated with polyclonal capturing Abs (Ab1). The second is a gold nanoparticle (NP) conjugated with a monoclonal recognition Ab (Ab2) and also hundreds of identical single-stranded DNA molecules of known sequence that pair with its complementary oligonucleotides through the hydrogen bonds from the Watson–Crick base-pairs. After forming a sandwich structure with the target of interest ([MMP-Ab1]-Target-[Ab2-NP-DNA]) and magnetic separation, the complementary DNAs are released by melting. Because of the known DNA sequence, these DNA strands are the barcodes that can be used as a unique identification tag for the target. Served as templates for the target, these bio-barcode DNAs can be amplified by the polymerase chain reaction (PCR) and detected by fluorescence [8,11]. Because of the use of PCR, the BBC assay is extremely sensitive for target detection [12]. Fig. 1 shows the basic principle of the BBC assay.

In our ABC assay, aptamers are used for target detection. Aptamers are small single-stranded DNAs that fold into 3D unique shapes by the Watson–Crick hydrogen bonds within the single-stranded DNA. Similar to Abs, aptamers have specific interaction with target molecules analogous to the Ab–Ag reaction [13,14]. Because of the high specificity, aptamers have been used clinically to treat disorders in human. For example, Macugen, a therapeutic aptamer against VEGF (vascular endothelial growth factor), is given to treat a common eye disease (macular degeneration) in the old people [15]. In our ABC assay, aptamers are used to substitute the recognition antibody (Ab2) and the bio-barcode DNA in the BBC assay. Similar to the BBC assay, the release of aptamers from the sandwiches ([MMP-Ab1]-Target-[Aptamer]) after heating will be a reporter for the target. The signal strength of this barcode aptamer after DNA amplification in the ABC assay becomes a quantification indicator for the target molecules. In addition, we have employed a novel isothermal recombinase polymerase amplification (RPA) in this new assay to amplify the DNA signal at a constant temperature to avoid the requirement of thermal cycling (Fig. 1).

In this study, this new ABC assay was employed to determine the amount of Cyto-*c* in the culture medium released from the drug-sensitive and -resistant liver cancer cells after the exposure to potential anti-cancer drugs. Results from our study confirmed that our ABC assay is an effective approach to screen anti-cancer agents from herbal medicine.

2. Experimental

2.1. Reagents and apparatus

Anti-Cyto-*c* aptamer, with the sequence shown in Table 1, was synthesized from Tech Dragon Ltd. Protein A magnetic beads (NEB S1425S) were obtained from New England BioLabs. Anti-Cyto-*c* Ab was obtained from Santa Cruz Bio-technology. Polyphyllin D (PD) was from Shanghai Fine Chemical. Real-time PCR kit was purchased from Applied Biosystems. RPA kit TwistAmp™ Basic was purchased from TwistDx. Cyto-*c*, bovine serum albumin (BSA) and other reagents were from Sigma-Aldrich. JC-1 (5,5′,6,6′-tetrachloro-1,1′,3,3′-tetraethyl-benzimidazol-carbocyanine iodide) was purchased from Invitrogen and EvaGreen was obtained from Biotium.

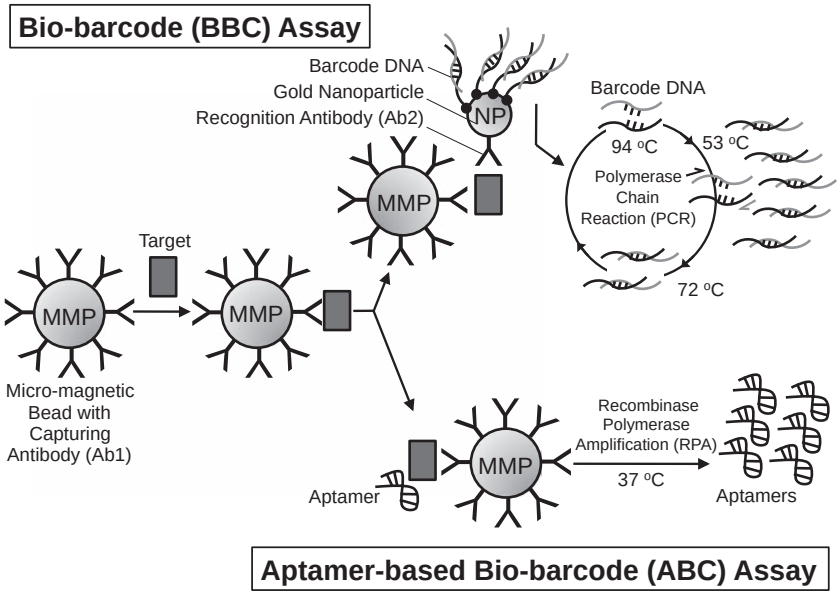

Fig. 1. Schematic diagram showing the BBC assay and the ABC assay for target detection. In the BBC assay, two types of particles are used. The first is a micro-magnetic particle (MMP) conjugated with antibodies (Ab1) against the target of interest and the second is a NP with another antibody (Ab2) specific to the same target using another epitope for binding. Also, the NP is coated with hundreds of single-stranded (ss) DNA of known sequence with its complementary DNA through the Watson–Crick base-pair annealing. Because of the known DNA sequence, these complementary strands or bio-barcode DNA can be used as a unique identification tag for the target. After mixing with analytes with the target of interest, sandwich structures ([MMP-Ab1]-Target-[Ab2-NP-DNA]) will be obtained by a magnetic field after repeated washings. With an increase in temperature to break the hydrogen bonds between the bio-barcode DNA and the ssDNA on the NPs from the sandwich complexes, the bio-barcode DNA strands are released into supernatant. These bio-barcode strands act as a template for DNA amplification by PCR. The amount of amplicons can then be determined by different DNA detection methods (upper panel). In the ABC assay, aptamers specific to the target are used to replace the NPs. In the sandwich structures, the aptamer serves as both the recognition Ab for the target and the bio-barcode reporter. In this modified ABC assay, the apatmer signal is amplified by the isothermal RPA (lower panel).

Table 1
DNA Sequence of the Aptamer and Primers for the PCR and RPA Assay.

Name	Sequence 5′-3′
Anti-Cyto-*c* aptamer	ATCGATAAGCTTCCAGAGCCGTGTCTGGGGCCGACCGGCGCATTGGGTACGTTGTTGCCGTAGAATTCCTGCAGCC
Forward primer for RT-PCR	ATCGATAAGCTTCCAGAG
Reverse primer for RT-PCR	GGCTGCAGGAATTCTACG
Forward primer for RPA	GAATTCTTCTAGAGATCGATAAGCTTCCAG
Reverse primer for RPA	CTGCATACTAGTAGGCTGCAGGAATTCTACG

2.2. Aptamer-based bio-barcode assay

Protein A magnetic beads were conjugated with mouse anti-Cyto-*c* Ab at 4 °C overnight. To generate a standard curve, the beads after washing with binding buffer (10 mM HEPES, 75 mM NaCl, 5 mM $MgCl_2$, 1 mM $CaCl_2$, pH 7.4) were incubated with Cyto-*c* of various concentrations in RPMI medium with 10% (v/v) fetal calf serum (FCS) for 1 h at 25 °C. Aptamers (400 pmol) was added and incubated for one more hour at 25 °C. After washing, all the aptamers were subject to the RPA.

2.3. RPA DNA amplification

The kit (TwistAmp™ Basic) from TwistDc for RPA amplification provides the uvsX recombinase, uvsY, gp32 single-strand DNA binding protein, Sau polymerase, ATP and dNTP. In the RPA, at least 30 bp-long primers are required to allow the recombinase to bind to. Therefore, conventional PCR primers cannot be used in the RPA DNA amplification. Extended primers were designed and used in this study (Table 1). After DNA amplification, amplicons were sequenced and the results showed perfect concordance with the sequence of the aptamer.

Mg^{2+} ion is a critical factor to initial DNA amplification in the RPA and its concentration is correlated to the rate of reaction. Although more Mg^{2+} added increases the amplification rate, excess amount of Mg^{2+} causes non-specific amplification. Mg^{2+} of 12 mM was found to be the optimal concentration to generate results with the highest signal-to-noise ratio (data not shown).

For the real-time RPA assay, the amount of aptamer so generated by RPA against time was reported by the fluorescence of EvaGreen DNA binding dye. The following formula was used for signal normalization: [Sample Fluorescence—Control Fluorescence]/[Baseline Fluorescence]. Baseline fluorescence was recorded at the first 5 min in the real-time the assay. The normalization step allows us to compare the results among assays.

2.4. Cell culture and apoptosis induction

Mimicking the clinical scenario for drug resistance development, drug-resistant hepatocellular carcinoma *R*-HepG2 were obtained from HepG2 cells (from ATCC (American Type Culture Collection)) after a continuous exposure to step-wise increasing concentrations of doxorubicin, a common anti-cancer drug used in hospitals, for at least 3 months. The LC50 (the concentration of a chemical that kills 50% of cell population) of doxorubicin in *R*-HepG2 is >200 μM [16]. Both the HepG2 and *R*-HepG2 were cultured in RPMI 1640 medium supplemented with 10% FCS (Gibco) at 37 °C, 5% CO_2. To maintain the doxorubicin-resistance, *R*-HepG2 cells were cultured with 1.2 μM doxorubicin during passages. For the induction of cell death, cells (1×10^6/mL) were treated with PD at the concentration as indicated at 37 °C, 5% for 24 h. Culture medium was then collected, centrifuged at 1500*g* for 5 min to remove debris and stored at 4 °C.

2.5. Assessment of apoptosis

Cell viability was measured by the MTT (3-(4,5-dimethylthiazol-2-yl)-2,5-diphenyltetrazolium bromide) assay for the mitochondrial dehydrogenase activity. HepG2 or *R*-HepG2 cells (2×10^4/well) were incubated in a 96-well plate with PD at 37 °C, 5% CO_2 for 24 h. MTT (final concentration 0.8 mg/mL) was then added to the wells for 2 h at 37 °C. Subsequently, the medium containing MTT was removed, and 100 μL of DMSO added. Absorbance was then measured at 540 nm with a plate reader (BioRad).

Flow cytometry was used to detect the collapse of mitochondrial trans-membrane potential ($\Delta\Psi_m$) for apoptosis by JC-1 [17]. JC-1 selectively enters the mitochondria, where it forms monomers when the $\Delta\Psi_m$ is relatively low. After excitation at 488 nm, the JC-1 monomers emit green fluorescence. At high $\Delta\Psi_m$, JC-1 forms aggregates and gives red fluorescence after excitation. The ratio between green and red fluorescence provides an estimate of $\Delta\Psi_m$ that is independent of the mitochondrial mass. Briefly, cells (2.5×10^5/mL) after treatment were washed with PBS and incubated with JC-1 (final concentration: 1 μg/mL) for 30 min at 37 °C. Cells were then washed with PBS three times to remove the JC-1 residues. Subsequently, changes in JC-1 signals from cells were determined by flow cytometry (FACScan, Becton Dickinson). Cell debris, characterized by a low forward scatter/side scatter, was excluded from analysis. Green and red fluorescence were detected with an excitation at 488 nm. For one single analysis, the fluorescence properties of 10,000 cells within gates were collected for analysis.

Standard SDS-PAGE with 15% polyacrylamide gel was performed for Western blot analysis. Proteins separated were electro-blotted onto a PVDF (poly vinylidene fluoride) membrane. Cyto-*c* was subsequently probed with the rabbit anti-Cyto-*c* primary Ab (dilution: 1:200) and anti-rabbit secondary Ab conjugated with horseradish-peroxidase (1:5000). Cyto-*c* was then detected by enhanced chemiluminescence method (Amersham). Protein band intensities were analyzed using the median border method (ImageJ software, version 10.2).

2.6. Statistical analysis

Results are mean $\pm$ SD from at least three independent assays. All of the experimental results were analyzed by Student's *t*-test, *p*-values less than 0.05 were considered statistically significant.

3. Results and discussion

3.1. Experimental principle

Fig. 1 shows the operation of the original BBC and our ABC assay. In our previous study, we isolated a 76-mer monoclonal aptamer for Cyto-*c* through 15 rounds of SELEX (Systematic Evolution of Ligands by Exponential Enrichment) to detect Cyto-*c* by PCR [14]. The major drawbacks of this approach are its long running time and requirement of thermal cycling to amplify the aptamer signals. To increase the simplicity and feasibility of the

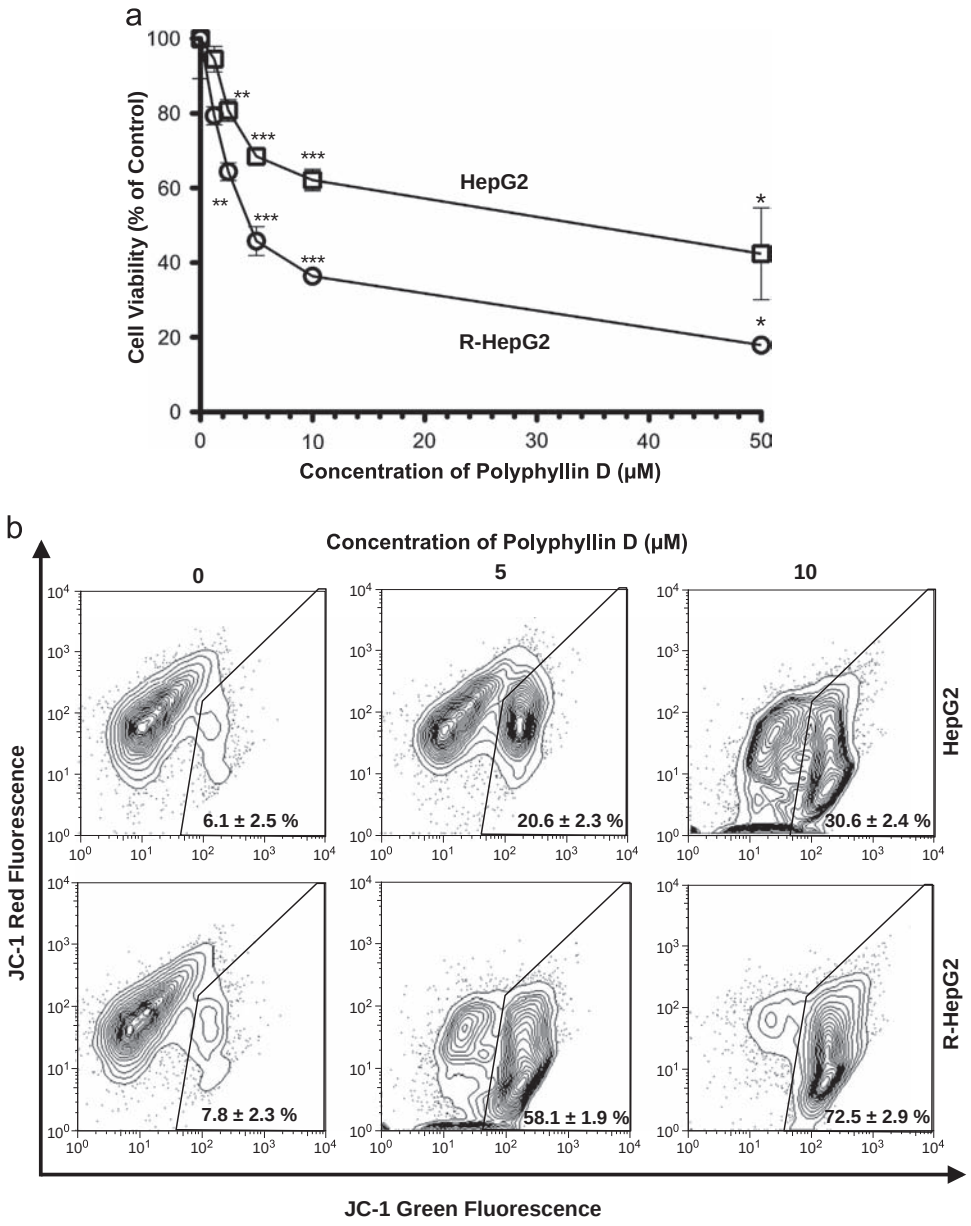

Fig. 2. Effect of Polyphyllin D on the viability and mitochondrial membrane potential in HepG2 and *R*-HepG2 cells. Cells (1×10^6/mL) were cultured with various concentrations of PD at 37 °C, 5% CO_2 for 24 h. Drug sensitivity was then measured by MTT assay after drug exposure (a). Results are mean ± SD from three independent assays. $^{*}P < 0.05$, $^{**}P < 0.01$, $^{***}P < 0.001$. Cells after treatment in (a) were labeled with JC-1 at 37 °C for 30 min. After washing, cells were submitted to flow cytometric analysis for the JC-1 red and green fluorescence (b). Numbers in the selected region represent the percentage of cells with depolarized $\Delta\Psi_m$ in the total population. Results are mean ± SD ($n=5$). (For interpretation of the references to color in this figure legend, the reader is referred to the web version of this article.)

ABC assay, we utilized a novel isothermal DNA amplification called RPA to substitute the PCR to amplify the aptamer signals at one single temperature (37 °C) without thermal cycling. To prove the concept, we first employed this modified ABC assay to study the effect of PD on the induction of cell death in a drug-sensitive and -resistant hepatocellular carcinoma line. In our previous studies, we have documented that *R*-HepG2, derived from its parental cells HepG2 after an *in vitro* selection of surviving cells in the continuous presence of a well-known chemotherapeutic agent doxorubicin, carries the features of MDR. The doxorubicin resistance was accompanied by cross-resistance to other anti-cancer drugs such as taxol and cisplatin as a result of the expression of *p*-glycoproteins that pump the toxic anti-cancer drugs out of the cells [16,18,19]. These cell lines are therefore an ideal *in vitro* system mimicking the acquired clinical MDR for drug screening.

As shown in Fig. 2a, it was found by using the MTT assay that PD was able to reduce the mitochondrial dehydrogenase activity in both the HepG2 and *R*-HepG2 cells in a dose-dependent manner with an IC50 (5 μM) in the *R*-HepG2 cells and 40 μM in the HepG2 cells, indicating that PD is able to bypass the MDR and kills more *R*-HepG2 cells. In the MTT assay, the metabolically inactive cells cannot be discriminated from the dead cells [20]. To eliminate this shortcoming, degree of mitochondrial damage in terms of depolarization of the $\Delta\Psi_m$ was measured by flow cytometry with JC-1 [17]. As shown in Fig. 2b, a dose-dependent loss of $\Delta\Psi_m$ was observed in the HepG2 and *R*-HepG2 cells after the challenge of cells with PD as evidenced by an increase in the cell number with high JC-1 green fluorescence. From the contour plots, it is clear that the effect of PD on the depolarization of $\Delta\Psi_m$ was stronger in the *R*-HepG2 cells (Fig. 2b). The percentage of cells with depolarized $\Delta\Psi_m$ (within the selected region defined by the

positive control staurosporine (data not shown)) increased from 6.1% of control cells to 20.6% (5 μM) and 30.6% (10 μM) of the PD-treated HepG2 and 7.8%, 58.1% and 72.5% in the *R*-HepG2 cells under the same conditions. These observations indicate again that the drug-resistant *R*-HepG2 cells were more sensitive to PD than the drug-sensitive HepG2 cells. These observations are in agreement with our pervious findings [18,19].

3.2. Detection of apoptosis by the release of Cyto-*c*

It has been known for a while that release of Cyto-*c* from the inter-membrane space of mitochondria is regarded as "a point of no return" for the apoptosis after $\Delta\Psi_m$ depolarization [5,21] and its release is an early apoptotic event and can be found in patients' blood or culture medium after chemotherapy [3,18,19]. Cyto-*c* in the medium is therefore a good candidate to report cancer death for drug screening. Fig. 3 shows the conventional assays to determine the Cyto-*c* in the culture medium by Western blot analysis (Fig. 3). Cyto-*c* of known concentration in standards (0–10^5 ng/mL) showed a dose-dependent effect in the Western blot analysis (Fig. 3). It is also clear that Cyto-*c* was released into the cultural medium from both the *R*-HepG2 and HepG2 cells after PD treatment. However, it is difficult to judge if the *R*-HepG2 cells released more Cyto-*c* than the HepG2 cells in Fig. 3. Moreover, this assay is tedious and time consuming. For example, it took more than 8 h to complete the Western blot analysis.

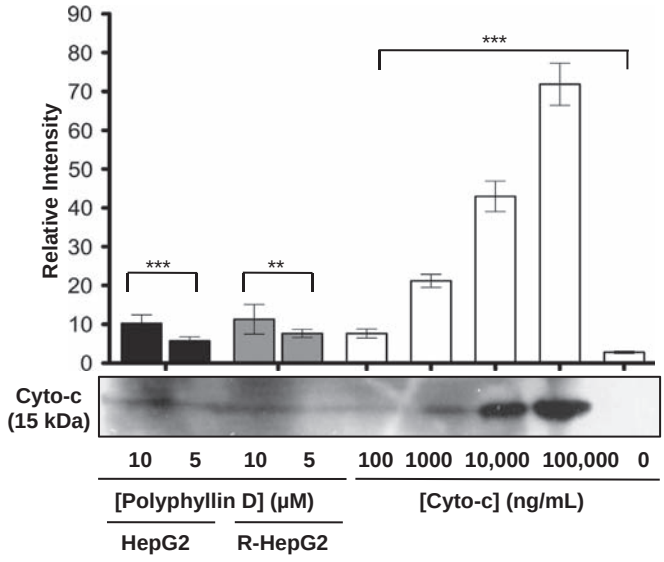

Fig. 3. Detection of Cyto-*c* by Western blot analysis. Cyto-*c* standards (0–100,000 ng/mL) and the Cyto-*c* released into the culture medium of cells after drug PD treatment at the concentration as indicated for 24 h at 37 °C, 5% CO_2 were subject to the SDS-PAGE and Western blot analysis. Relative intensity was measured by ImageJ and shown in the bar chart. Results are mean ± SD ($n=3$), $^{**}P<0.01$, $^{***}P<0.001$.

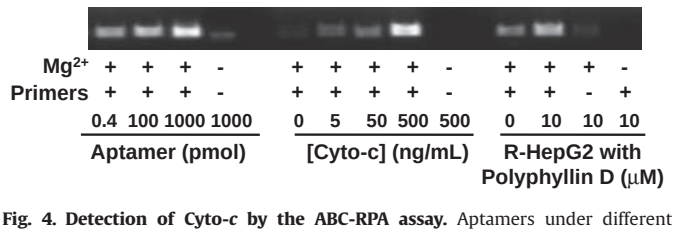

Fig. 4. Detection of Cyto-*c* by the ABC-RPA assay. Aptamers under different settings as indicated were amplified by the isothermal RPA in the presence or absence of Mg^{2+} (12 mM) and primers and subject to gel electrophoresis. Lanes 1–4 (from the left hand side) were used to assess the ability of RPA to amplify the Cyto-*c* specific aptamer. ABC assay was used to detect the aptamers associated with the Cyto-*c* standards 0–500 ng/mL (Lane 6–10). The ABC assay was also used to evaluate the amount of Cyto-*c* released from the *R*-HepG2 cells after PD treatment at the dose as indicated for 24 h (Lane 12–15).

3.3. Detection of Cyto-*c* with ABC-RPA assay

Next, we employed our ABC assay using the RPA to amplify the aptamer signals to screen potential anti-cancer drugs. RPA is a novel isothermal DNA amplification method that operates at one single temperature at 37 °C. The chemistry of RPA is different from that of PCR on DNA amplification. During RPA, melting of the double-stranded DNA is not required for the primers to bind to their complementary target sequences. RPA is initiated by a cofactor Mg^{2+} when bound to the RPA polymerase. During the

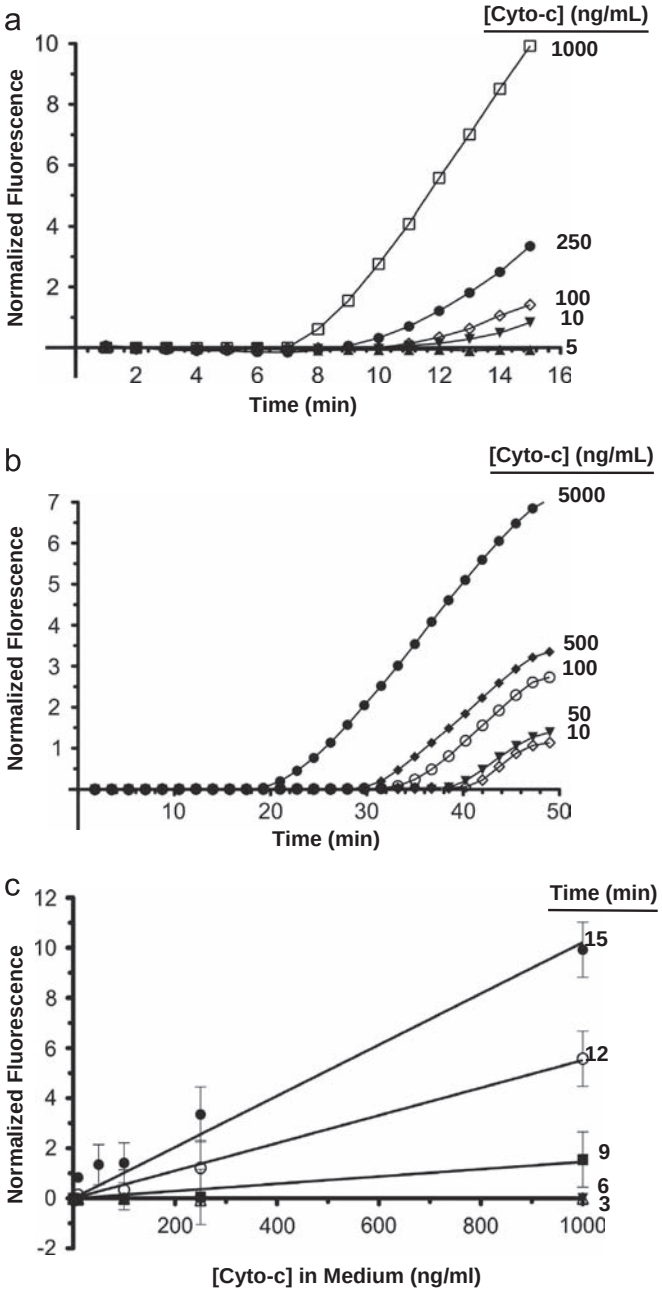

Fig. 5. Detection of Cyto-*c* by real-time RPA and real-time PCR. Cyto-*c* standards as shown in the figure were used for the assays. The aptamer reporter was subject to the RPA (a) or PCR (b) amplification. Panel (c) shows the standard curves of the aptamer signals from the Cyto-*c* standards (0–1000 ng/mL) at 3, 6, 9, 12, 15 min. Results are mean ± SD from three independent assays.

RPA process, the recombinase untwists and separates the double-stranded DNA, and allows the primers to bind to their corresponding target sequence and at the same time the displaced DNA strand is stabilized by the single-stranded DNA binding proteins. After initiating the chemical reaction by the addition of Mg^{2+}, the primer-recombinase complex starts DNA elongation based on the DNA sequence in the template to generate DNA copies [22].

Fig. 4 shows an end-point detection for the aptamers from different samples amplified by the RPA for 30 min. These samples included the stock aptamer of different known concentrations, aptamers associated with Cyto-*c* standard of different amount and the Cyto-*c* released from cells after PD treatment. As can be seen in the electrophoresis gel photo (Fig. 4), no DNA band was found in the gel when Mg^{2+} and primers were omitted in the reaction mix indicating that both the Mg^{2+} and primers are required for the DNA amplification. The weak signal in Lane 4, in the absence of Mg^{2+} and primers, was the read-out generated by the aptamers (1000 pmol) added in the system. With the supply of Mg^{2+} and primers for the RPA, the DNA aptamer signal was greatly enhanced in a dose-dependent manner (Lane 1–3). This dose-dependent results were obtained from the aptamers associated with the Cyto-*c* standards with increasing concentration (Lane 6–10). Also, PD was able to release the Cyto-*c* from the *R*-HepG2 cells into the medium and signals were generated by the RPA (Fig. 4, the last 4 lanes). To have a better measurement, we repeated the experiments with the real-time RPA assay to monitor the amount of Cyto-*c* released in the medium.

3.4. Cyto-c quantitation by real-time RPA

Fig. 5a shows the real-time RPA profile using EvaGreen to construct a standard curve for the Cyto-*c* aptamer from five Cyto-*c* samples of known concentration. From the profile, it is clear that the aptamer signals started to increase 7 min after the addition of Mg^{2+} from the 1000 ng/mL Cyto-*c* sample. Also, the detection limit using our aptamer to probe Cyto-*c* was found to be 10 ng/mL at the 15-min time point (Fig. 5a). For comparison, real-time PCR with thermal cycling was used to repeat the assay (Fig. 5b). As can be seen, PCR showed similar detection limit but it took more than 30 min to show the positive results. Also, the slope of curve from the real-time RPA was much steeper than that of the PCR (Fig. 5a and b). Using our ABC approach, we obtained standard curves and the one with 15-min amplification showed a steep slope and a good linear relationship ($y=0.0096x+0.46$, where R square value equals to 0.986) (Fig. 5c). Next, we used this standard curve to determine quantitatively the Cyto-*c* released into the medium from the HepG2 and *R*-HepG2 cells after the treatment with doxorubicin and PD by the ABC assay (Fig. 6). Cyto-*c* from the control groups without drug treatment was found below 50 ng/mL. As expected, doxorubicin released much more Cyto-*c* from the HepG2 (550 ng/mL at 10 μM) than the *R*-HepG2 cells (50 ng/mL at 10 μM), while PD was found to release less Cyto-*c* from the HepG2 cells (410 ng/mL at 10 μM) than the *R*-HepG2 (580 ng/mL at 10 μM) in the medium (Fig. 6 and Table 2). Collectively, our results indicate that our new ABC assay was sensitive enough to detect the Cyto-*c* leakage in the culture medium after drug treatment.

Table 2
Anti-cancer drug screening by the ABC Assay.

Drugs	Dose (μM)	[Cyto-*c*] (ng/mL)	
		HepG2	*R*-HepG2
Polyphyllin D	5	300 ± 50 (IC50 = 30 μM)	460 ± 50 (IC50 = 4 μM)
	10	410 ± 60 (IC50 = 30 μM)	580 ± 60 (IC50 = 4 μM)
Doxorubicin	10	550 ± 60 (IC50 = 7 μM)	50 ± 30 (IC50 > 200 μM)
Berberine	30	650 ± 10 (IC50 = 4 μM)	400 ± 90 (IC50 > 50 μM)
Crucumin	10	570 ± 100 (IC50 = 6 μM)	150 ± 50 (IC50 = 30 μM)
Ferutinin	30	760 ± 100 (IC50 < 3 μM)	550 ± 50 (IC50 = 40 μM)
Betulinic acid	30	1100 ± 70 (IC50 < 3 μM)	850 ± 50 (IC50 = 30 μM)

Cells (1×10^6/mL) were cultured with the agents at the concentration as indicated for 24 h at 37 °C, 5% CO_2. The amount of Cyto-*c* released into the culture medium was then determined by the ABC assay. Results are mean ± SD from three independent assays. The IC50 of the agent for the HepG2 and *R*-HepG2 cells was also shown for reference.

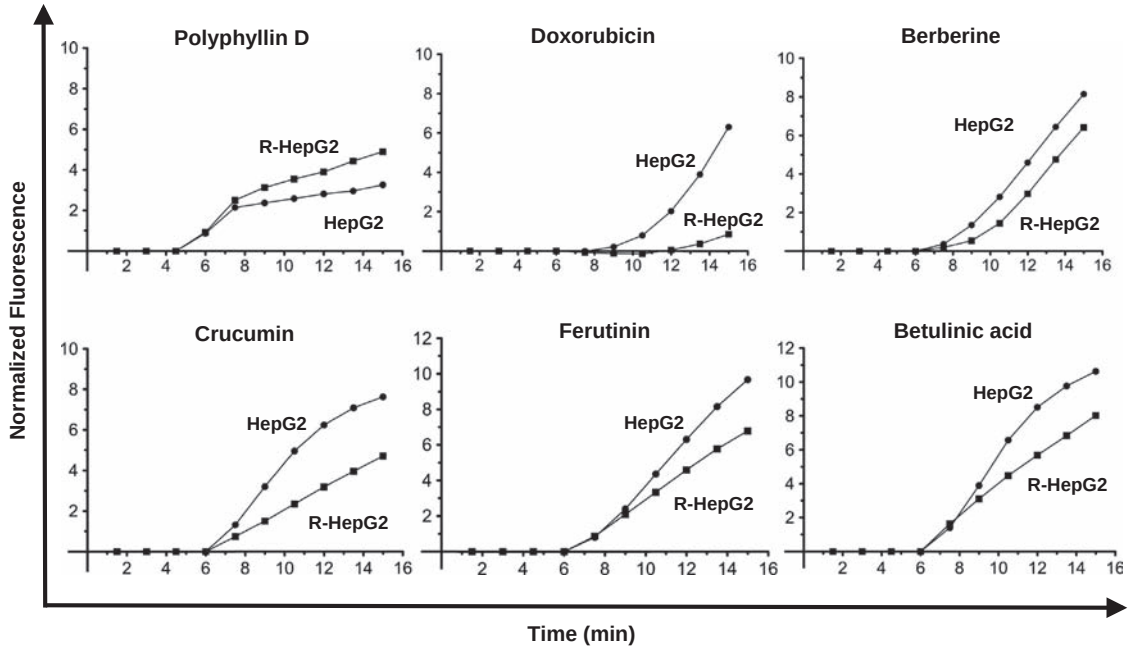

Fig. 6. Detection of Cyto- *c*by real-time RPA to determine the Cyto- *c*in the culture medium of HepG2 and *R*-HepG2 cells treated with different agents. Cells (1×10^6/mL) were cultured with the agents of concentrations as indicated (Polyphyllin *D* (5 μM), Doxorubicin (10 μM), Berberine (30 μM), Crucumin (10 μM), Ferutinin (30 μM), Betulinic acid (30 μM)) at 37 °C, 5% CO_2 for 24 h. One mL of culture medium from each treatment was then subject to the ABC assay and the aptamer signals were determine by the real-time RPA with EvaGreen at 37 °C. Panels are typical results from 3 independent assays.

3.5. Drug screening with the ABC-RPA detection assay

To test the utility of our ABC assay, four more drug candidates selected by literature survey were used to treat the HepG2 and *R*-HepG2 cells. These four agents were berberine, curcumin, ferutinin, and betulinic acid. All four agents have been reported to show anti-cancer activities in different types of cancer. Berberine induced mitochondrial fragmentation and decreased the ATP level in the K1735-M2 mouse melanoma cells [23]. Curcumin caused mitochondrial hyperpolarization and mitochondrial DNA damage in HepG2 cells [24]. Ferutinin promoted mitochondrial calcium overload in human colon cancer and human Jurkat T cells [25,26] while betulinic acid directly triggered mitochondrial permeability transition in the HepG2 cells [27,28].

Fig. 6 shows the read-out from the real-time ABC assay using the RPA for signal amplification to test for their cancer killing effect. As can be seen, all the agents produced positive signals 6 min after the RPA reaction. In depth examination of these curves indicate that these agents released more Cyto-*c* from the HepG2 than that in the *R*-HepG2 cells, indicating that these agents could not bypass the MDR in the *R*-HepG2 cells (Fig. 6). Table 2 gives a summary for the Cyto-*c* released from the HepG2 and *R*-HepG2 cells quantitatively using our ABC assay approach, as well as the IC50 from the MTT assay after treatment with these four agents. Again, none of these agents besides PD could induce a stronger Cyto-*c* release from the *R*-HepG2 than the HepG2 cells.

4. Conclusion

We have demonstrated that our new ABC assay using RPA is a robust, selective, simple (using one temperature at 37 °C for signal amplification) and fast (process can be completed within 3 h) method for anti-cancer drug screening through the detection of Cyto-*c*. As suggested by a feature report from the US National Academy of Sciences entitled "Toxicity Testing in the 21st Century: A Vision and a Strategy" in 2007, investigators are recommended to use cell lines or human cells and mechanism-based assays to replace traditional animal testing for drug screening and toxicity evaluation (http://www.nap.edu/openbook.php?record_id=11970&page=1). Our ABC assay is a starting point along this direction and we anticipate that more assay formats will be developed for the anti-cancer drug screening in the near future.

Acknowledgement

This work is supported by a GRF Grant (413310) and a CRF grant (CUHK1/CRF/12G) from the Hong Kong Special Administrative Region.

References

[1] C.F. Higgins, Nature 446 (2007) 749–757.
[2] K.M. Debatin, D. Poncet, G. Kroemer, Oncogene 21 (2002) 8786–8803.
[3] A. Osaka, H. Hasegawa, Y. Yamada, K. Yanagihara, J. Cancer Res. Clin. Oncol. 135 (2009) 371–377.
[4] A. Renz, W.E. Berdel, M. Kreuter, C. Belka, K. Schulze-Osthoff, M. Los, Blood 98 (2001) 1542–1548.
[5] C. Garrido, L. Galluzzi, M. Brunet, P.E. Puig, C. Didelot, G. Kroemer, Cell Death Differ. (2006) 1423–1433.
[6] A. Osaka, H. Hasegawa, K. Tsuruda, N. Inokuchi, K. Yanagihara, Y. Yamada, M. Aoyama, T. Sawada, S. Kamihira, Int. J. Lab. Hematol. 31 (2009) 307–314.
[7] K.C. Leung, H.P. Ho, Y.W. Kwan, S.K. Kong, Expert Rev. Mol. Diagn. (2010) 863–867.
[8] J.M. Nam, C.S. Thaxton, C.A. Mirkin, Science 301 (2003) 1884–1886.
[9] J.M. Nam, K.J. Jang, J.T. Groves, Nat. Protoc. 2 (2007) 1438–1444.
[10] J.M. Nam, S.I. Stoeva, C.A. Mirkin, J. Am. Chem. Soc. 126 (2004) 5932–5933.
[11] D.G. Georganopoulou, L. Chang, J.M. Nam, C.S. Thaxton, E.J. Mufson, W.L. Klein, C.A. Mirkin, Proc. Natl., Acad. Sci. U.S.A. 102 (2005) 2273 2266.
[12] D.A. Giljohann, C.A. Mirkin, Nature 462 (2009) 461–464.
[13] A.D. Ellington, J.W. Szostak, Nature 346 (1990) 818–822.
[14] I.P. Lau, E.K. Ngan, J.F. Loo, Y.K. Suen, H.P. Ho, S.K. Kong, Biochem. Biophys. Res. Commun. 395 (2010) 560–564.
[15] P.R. Bouchard, R.M. Hutabarat, K.M. Thompson, Annu. Rev. Pharmacol. Toxicol. 50 (2010) 237–257.
[16] J.Y. Cheung, R.C. Ong, Y.K. Suen, V. Ooi, H.N. Wong, T.C. Mak, K.P. Fung, B. Yu, S.K. Kong, Cancer Lett. 217 (2005) 203–211.
[17] A. Cossarizza, M. Baccarani-Contri, G. Kalashnikova, C. Franceschi, Biochem. Biophys. Res. Commun. 197 (1993) 40–45.
[18] R.K.Y. Lee, R.C.Y. Ong, J.Y.N. Cheung, Y.C. Li, J.Y.W. Chan, M.M.S. Lee, Y.K. Suen, K.P. Fung, H.P. Ho, B. Yu, M. Li, T.T. Kwok, S.K. Kong, Curr. Chem. Biol. 27 (2009) 409–419.
[19] R.C. Ong, J. Lei, R.K. Lee, J.Y. Cheung, K.P. Fung, C. Lin, H.P. Ho, B. Yu, M. Li, S.K. Kong, Cancer Lett. 261 (2008) 158–164.
[20] T. Mosmann, J. Immunol. Methods 65 (1983) 55–63.
[21] M.L. Lim, M.G. Lum, T.M. Hansen, X. Roucou, P. Nagley, J. Biomed. Sci. 9 (2002) 488–506.
[22] O. Piepenburg, C.H. Williams, D.L. Stemple, N.A. Armes, PLoS Biol. 4 (2006) e204.
[23] G.C. Pereira, A.F. Branco, J.A. Matos, S.L. Pereira, D. Parke, E.L. Perkins, T.L. Serafim, V.A. Sardão, M.S. Santos, A.J. Moreno, J. Holy, P.J. Oliveira, J. Pharmacol. Exp. Ther. 323 (2007) 636–649.
[24] J. Cao, Y. Liu, L. Jia, H.M. Zhou, Y. Kong, G. Yang, L.P. Jiang, Q.J. Li, L.F. Zhong, Free Radic. Biol. Med. 43 (2007) 968–975.
[25] A. Macho, M. Blanco-Molina, P. Spagliardi, G. Appendino, P. Bremner, M. Heinrich, B.L. Fiebich, E. Muñoz, Biochem. Pharmacol. 68 (2004) 875–883.
[26] F. Poli, G. Appendino, G. Sacchetti, M. Ballero, N. Maggiano, F.O. Ranelletti, Phytother. Res. 19 (2005) 152–157.
[27] A. Szuster-Ciesielska, M. Kandefer-Szerszeń, Pharmacol. Rep. 57 (2005) 588–595.
[28] Y. Li, K. He, Y. Huang, D. Zheng, C. Gao, L. Cui, Y.H. Jin, Mol. Carcinog. 49 (2010) 630–640.